Creep-Rupture Characteristics of Type 304 Stainless Steel Weldments with Type 308 Stainless Steel Welds at 1100°F

Testing is carried out on specimens sufficiently large and designed to simulate the constraint of a circumferential weld of pipe or a pressure vessel

BY M. J. MANJOINE

ABSTRACT. This paper describes the creep of Type 304 stainless steel plate weldments as influenced by the level of ferrite and the geometries of the Type 308 stainless steel weld metal. The method of testing enabled multiple determinations of the strains for weld metal, heat-affected zone (HAZ), and base metal at crack initiation and rupture.

The tests of weldments included two levels of ferrite, 2 FN and 9 FN, and two weld geometries—75 deg V-groove weld and a single, square groove weld made from one side with a backing plate at the weld root. All tests were performed at 24 ksi (165 MPa) and 1100°F (593°C). The weldments with a central axial weld and constraints at the ends of the gage section were tensile loaded. Therefore, all zones of the weld are subjected to the same overall axial deformation. This loading and constraint is similar to a circumferential weld in a pipe or vessel.

The failure mode was a function at all three of the following:

1. The relative strengths and ductilities of the weld metal, heat-affected zone (HAZ) and the base metal.
2. The residual stresses and deformations from the welding process.
3. The stress and strain histories under loading.

The low-ferrite Type 308 stainless steel weld metal has the highest strength and lowest ductility as compared to the high-ferrite Type 308 stainless steel weld metal and the base metal. The tensile stresses from applied loads and residual strains are highest in the weld metal on the crown face. Therefore, crack initiation occurred in the weld metal on the crown face at about 50% of rupture life. The axial creep strain after stress redistribution at this location was about 4.8% for crack initiation. The V-groove weld geometry required a longer time for crack propagation from crown to root and then, transversely, through the base metal than that for the square groove weld.

The high-ferrite weld metal has a lower strength and higher ductility than those of the low-ferrite weld metal and a higher strength and lower ductility than the base metal. Crack initiation occurs in the HAZ at the weld root face where the metallurgical notch has a high constraint. The local strain at crack initiation was about 7% at about 36% of life. The crack propagation through the HAZ from the weld root to crown face required an additional 34% of life. The average rupture lives of the high ferrite welds were about 20% longer than those for the low-ferrite welds.

In terms of actual rupture life, the minimum crack initiation time of any of these weldments was greater than the rupture time for the Type 304 stainless steel base metal that is used to set the ASME code design life.

Paper presented at the 65th Annual AWS Convention in Dallas, Texas, during April 9-13, 1984, under sponsorship of the Metal Properties Council.

M. J. MANJOINE is a Consultant for the Westinghouse Research and Development Center, Pittsburgh, Pennsylvania.

Introduction

The Task Group on "Properties of Weldments for Pressure Service" of Subcommittee 1 of the Metal Properties Council is conducting a comprehensive program to determine the effect of weld metal Ferrite Number (FN) of the Type 308 stainless steel weld metal on the creep-rupture characteristics of Type 304 stainless steel weldments. Prior work consisted of individual efforts by members of the Task Group and a sponsored program on weld metal properties at Battelle-Columbus Laboratories (Ref. 1).

This paper summarizes the research on the creep-rupture characteristics of weldments prepared with a low- and high-ferrite in the Type 308 stainless steel weld metal and for weld configurations simulating V- and square-groove geometries. These are identified here as a V-groove weld or a square-groove weld. The method of testing is novel in that the specimen is sufficiently large and designed to simulate the constraint of a circumferential weld of a pipe or pressure vessel. In addition, the gage section is premarked with a grid, which allows the measurement of strains from photographs made at interruptions of the test (Ref. 2). Analyses of these measurements and photographs enabled an understanding of the initiation and propagation of damage and cracking.

Materials

Weld Metal

The Task Group supervised the preparation of the weld metals from covered electrodes to produce the levels of ferrite and chemistry desired. The weld metals were produced by Arcos Corporation under the supervision of R. D. Thomas, Jr. (Ref. 3). The metal weld electrodes utilized in the weldments of this paper were from two levels of the range produced: extra-low ferrite, FN 2, and a medium ferrite, FN 9. They are identified here as "low-ferrite" and "high-ferrite" weldments, respectively.

The characterization of the weld metals was performed by Battelle-Columbus Laboratories (Refs. 1, 4) and included creep rupture and short-time tensile tests. Additional work was performed by the Oak Ridge National Laboratory and Combustion Engineering (Ref. 5).

Base Metal

The base metal was supplied by the Oak Ridge National Laboratory and was solution-annealed Type 304 stainless steel from reference heat 9T 2796. This heat has been well characterized (Ref. 6).

Weldments

Welding

A task force of the Metal Properties Council prepared the instructions for preparation of the plate edges, welding current, voltage and travel speed for all the welding. These instructions were the same as those used in preparing the weld metal pads for the program on the effect of weld metal ferrite (Refs. 1, 3). The weldments were then prepared by Oak Ridge National Laboratory (ORNL) under the direction of task force member D. P. Edmonds.

Butt joints were made with shielded metal arc welding, in two 0.5 in. (12.7 mm) thick annealed Type 304 stainless steel plates about 4 in. (102 mm) wide by 1.5 in. (38 mm) long. The weld interfaces were either (a) normal to the plate surface, or (b) involved conventional single V-groove preparation (75 deg included angle). The width of the weld metal on the weld face side was about the same for both welds at about 0.69 in. (18 mm)—Table 1.

The welds were radiographed by ORNL and again by Westinghouse to locate any discontinuities. The specimen blanks were machined from the discontinuity-free areas. A blank was 4 in. (102 mm) wide by 8.5 in. (216 mm) long with the centerline of the axial weld at the mid-width of the blank. Equal metal was machined from each face of the blank to produce a thickness, t, of ⅓ in. (8.5 mm).

After etching the blank to reveal the weld, it was dye-penetrant inspected and machined to center the weld in the gage section. The measurements made during the welding process are summarized in Table 1; they were:

1. Geometries of the joint preparations and machined welds.
2. Ferrite numbers, FN, from "Magna-Gage" readings.
3. Hardnesses at selected locations.

The ferrite measurements show the effect of base metal dilution at the roots of the V-groove welds. The ferrite number increased from the weld face to root face (1.9 FN to 2.6 FN) for the low-ferrite weld metal, but decreased for the high-ferrite weld metal (8.0 FN to 5.2 FN). An insignificant difference in ferrite number was noted for the square-groove welds where the dilution was less. The hardness was higher at the root face than at the weld face of any weld and was highest for high-ferrite weldments. The base metal hardnesses were slightly higher at a distance of 0.5 in. (12.7 mm) from the edge of the high-ferrite weldments than those for the low-ferrite ones.

After the crown faces were machined off, the V-groove welds were about three times as wide at the weld faces than at the root faces.

Test Specimen

The gage section of the specimen was ⅓ in. (8.5 mm) thick, t, by 3.33 in. (85 mm), 10t, in width and length. The faces were marked with a square grid of 20 lines per inch. The load was applied by welding extension pieces which sandwiched the blank beyond the gage section—Fig. 1.

The pins in Fig. 1 were used to align the extension pieces during welding of the socket areas and edges and also served as loading members. Unloaded reference strips were placed at each edge for calibration of measurements of photographs. Nine thermocouples were spot welded in noncritical areas to measure the temperature during the test. The etched weld material can be seen in Fig. 1 through the surface grid. The holes, in the extension pieces just beyond the gage section, position the overall extensometer used in the test.

The external load is applied at the ends of the extension pieces through holes which have been machined on the centerline of the weld and gage section. This geometry of test specimen with its high constraint at the heads causes equal average axial strain for all parts of the weldment and a decreasing lateral constraint to mid-length of the gage section. This constraint influences the ductilities of the zones of the weld because of the triaxiality of the stress and results in an axial strain increase up to mid-length (Ref. 7). Since the creep strain increases with time, multiple crack initiations can be observed and measured at the minimum ductility areas of the weldment (Ref. 7).

Table 1—Weld Pre-Test Data

ITEM		Specimen number 240	241	242	243
Weld type		V-groove	Square groove	V-groove	Square groove
Ferrite no.[a]	Nominal	2	2	9	9
Surface face		1.9	2.1	8.0	8.8
Root face		2.6	1.8	5.2	7.0
Weld joint configuration					
Included angle, deg		75	0	75	0
Root face, in. (mm)		0.06 (1.5)	—	0.06 (1.5)	—
Root opening, in. (mm)		0.09 (2.3)	0.69 (18)	0.09 (2.3)	0.69 (18)
Weld width at surface, in. (mm)		0.69 (18)	0.69 (18)	0.69 (18)	0.69 (18)
Machined joint[b]					
Root width, in. (mm)		0.2 (5.0)	0.48 (12)	0.18 (4.6)	0.55 (14)
Root hardness DPH[c]		232	246	255	267
Surface width, in. (mm)		0.62 (16)	0.49 (12)	0.6 (15)	0.55 (14)
Surface hardness DPH[c]		209	220	222	223
BASE METAL DPH[d]		168	172	190	180

(a) Average of 30 measurements along weld with Magna-Gage (by D. Edmonds, ORNL)
(b) Crown and backing plate machined off.
(c) Peak valve at center of weld, diamond pyramid hardness numbers—weld metal hardness for weld root and weld face.
(d) 0.5 in. from weld fusion line.

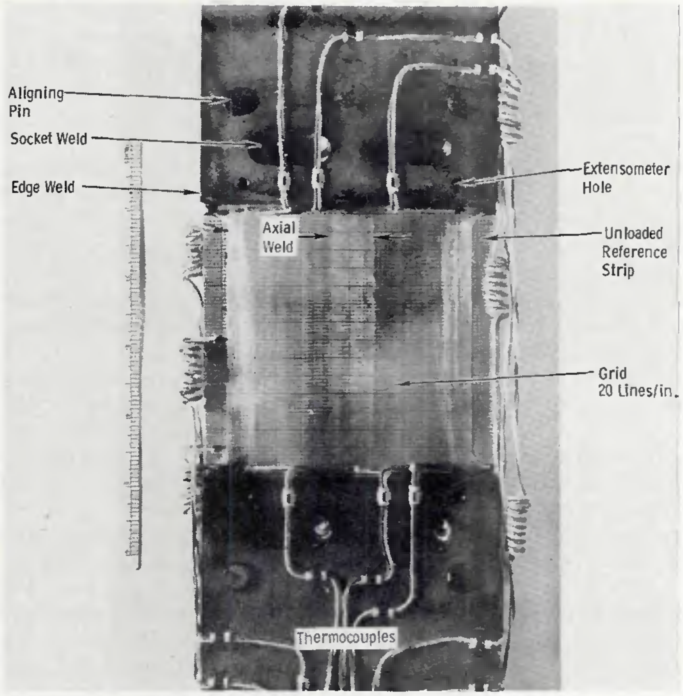

Fig. 1—Pre-test photograph of specimen 242 weld face

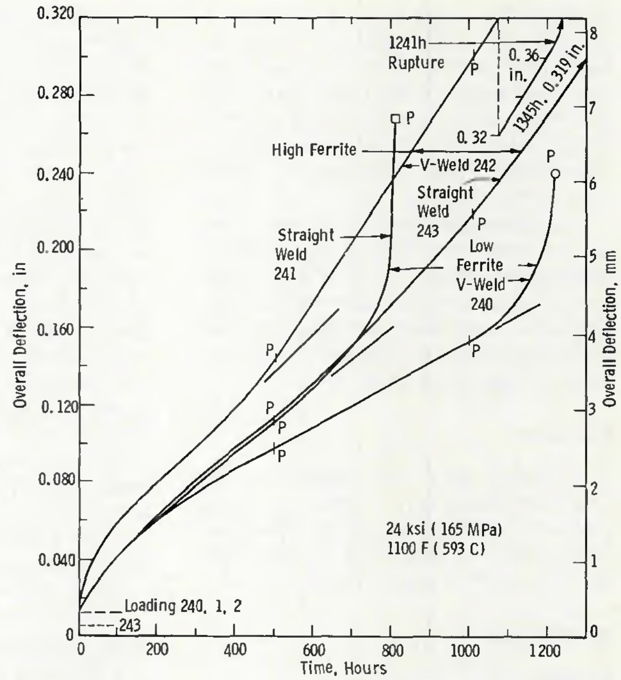

Fig. 2—Creep-rupture curves of welds (square groove and "straight" are the same)

Creep-Rupture Tests

All the creep-rupture tests were performed at a stress of 24 ksi (165 MPa) and 1100°F (593°C). From tests on Type 304 stainless steel welds (Ref. 8), the estimated life for these conditions was about 2000 hours (h). The testing was interrupted at 500 h intervals and when the overall extension rate indicated rapid crack growth rate.

Low-Ferrite Weldments—Weld Metal 2 FN

Specimen 240. The low-ferrite V-groove weld had the lowest deflection rate of all the specimens—Fig. 2. At 500 h, visual inspection (Fig. 4A) revealed four cracks about 3 mm (0.12 in.) apart in the weld metal on the weld face only. The longest was about 6 mm (0.24 in.) and near mid-length of the gage section. At 1000 h (Fig. 4B), the initial cracks had propagated half way across the weld metal on the weld face, and additional cracks had formed in the weld metal about 20 mm (0.79 in.) above mid-length.

Close inspection showed cracking, halfway across the weld on the root face, only at this location—Fig. 3A. At 1219 h the test was interrupted because of the rapid deflection rate—Fig. 2. Inspection (Fig. 4C) showed little growth of some of the initial cracks on the weld face. However, the crack about 20 mm (0.79 in.) above mid-length had grown across the weld metal and into the base metal on both faces—Figs. 3B and 4C. The estimated crack length was about 1 in. (25.4 mm).

Since rupture was imminent at the highest net section stress and since the crack was across the weld and HAZ, the creep-rupture test was considered to be complete. The load was reduced to 83% to investigate the crack growth rate in the base metal. This latter growth rate was nearly constant for the next 300 h, as estimated from the overall deflection rate (Table 2) and then accelerated to rupture in 561 h at the lower load—Fig. 4D and Table 2.

The axial strains were measured from the grid photographs and are shown as strain profiles along the length for two width positions:

1. 1 mm (0.04 in.) from the edge.
2. At the centerline of the axial weld—Fig. 5.

Although the overall deflection and the average strain are the same for the two positions, the strain profiles reflect the specimen and crack geometries. At 500 h the edge profile shows the strain concentration at the fillets and the decreasing strain to mid-length. The centerline profile at 500 h shows the increase in strain from the ends to mid-length and the distortion (Fig. 5) above mid-length due to the openings of the cracks (c, shown as vertical lines) with major crack width.

It is estimated that the cracks initiate (probably slightly subsurface) at about 4.8% strain. At 1000 h, the strain features

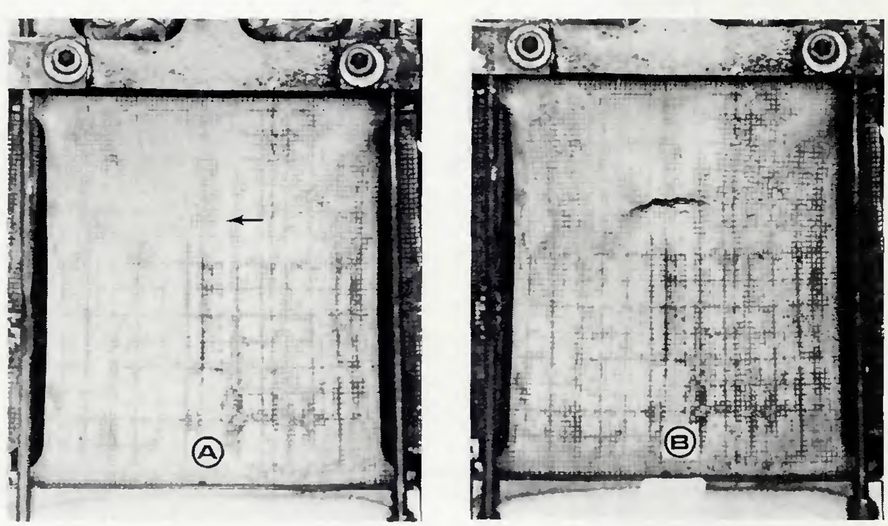

Fig. 3—Photographs of root face of low-ferrite V-groove weld, 240: A—1000 h; B—1219 h

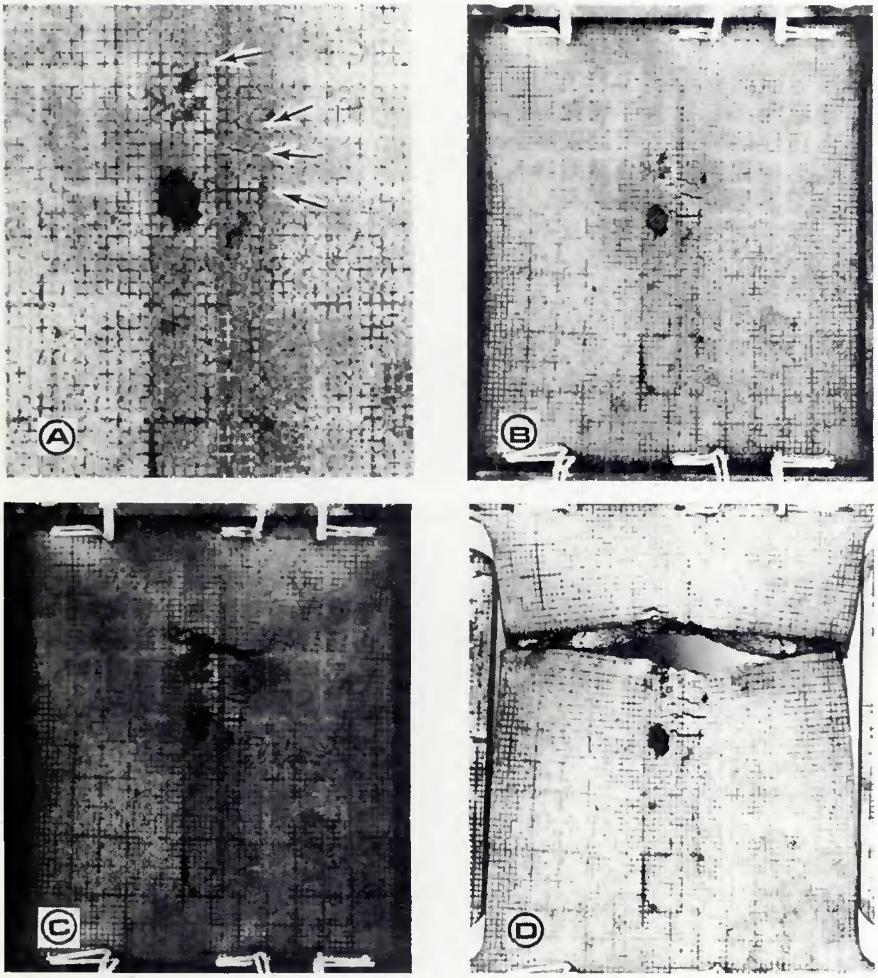

Fig. 4 — Weld face of low-ferrite V-groove weld, 240: A — 500 h, X2; B — 1000 h, X1; C — 1219 h, X1; D — rupture, X1 (reduced 50% on reproduction)

at the two width positions are increased. The "rupture" crack that developed through the weld thickness was at a position of 24% of length. Figure 3B shows that, after 1219 h, the cracks have propagated across the weld into the base metal.

The lateral contraction strain profiles are plotted in Fig. 6 at the length positions of the major cracks at 500 and 1000 h. The average negative strains at these times and at 1219 h are shown at the right edge. The crack length and width positions are also shown. The contraction strain is slightly higher at mid-width (at the weld). The ratio of the transverse to axial strain at the weld centerline for 500 h is −0.30, and the estimated transverse stress due to the lateral constraint is about 24% of the axial stress (Ref. 7).

Specimen 241. The minimum deflection rate (Table 2 and Fig. 2) for the low-ferrite straight weldment was 45% higher than that for the V-groove weld, even though in the cross section there is a greater volume of weld metal that is stronger than the base metal (Ref. 1). Inspection at 500 h revealed a single crack with a width of 1.5 mm (0.06 in.) in the weld metal on the surface face only at 49% of length — Fig. 7A. At 811 h, this crack had grown through the thickness of the weld metal and laterally into the base metal to a length of 38 mm (1.5 in.) — Fig. 7B.

Since rupture was imminent at this higher net section stress, the load was reduced to 50% to measure the displacement rate. This new rate was only about 4% of the minimum displacement rate at crack initiation. After a nearly constant rate for 480 h, the load was increased to 75% of initial load. The deflection rate increased for the next 27 h and then accelerated. Rupture occurred after 71 h at this final load — Table 2.

The axial strain profiles at the edge and centerline width positions are plotted in Fig. 8 for 500 h and rupture. The strain at the crack tip in the weld face of the weld metal was 4.8%, which is the same as that for the V-groove weld. The measured lateral contraction strain near the crack tip was −1.7%, and the estimated transverse stress was 19% of the axial stress. The transverse strain contour was very similar to that shown in Fig. 6 and is not shown here. At 500 h for the mid-length position of the crack, the peak transverse strain was −1.8%, and the average across the section was 1.54% for this low-ferrite straight-weldment.

High-Ferrite Weldments—Weld Metal 9 FN

The high-ferrite welds (Fig. 2) had slightly higher overall deflections at a given time, minimum deflection rates, rupture deflections and times for complete cracking across the weld metal (weld rupture time) — Table 2.

Specimen 242. The high-ferrite V-groove weld at 503 h (Fig. 9A) showed crack initiation at the HAZ on the root face only. The longest crack was only 0.2 mm (0.008 in.) and transverse to the load axis at 63% of the gage length. At 1009 h the cracking in this area (Fig. 9B) had increased in length to 1.6 mm (0.006 in.), and transverse cracks were observed from 28% to 78% of length with principal cracks about 4 mm (0.16 in.) apart. A few HAZ cracks were also observed at 1009 h on the weld face in the region of peak strain and the maximum length was about 0.5 mm (0.02 in.). Rupture occurred in 1241 h at the 63% length position — Fig. 9C. Many short HAZ cracks are visible near the fracture area on the weld face side — Fig. 9D.

In Fig. 2 it can be noted that the overall deflection rate increased 50% at about 450 h and remained nearly constant up to 1150 h. It is speculated that subsurface crack initiation occurred at 450 h. Additional cracking along the HAZ's form with time and propagation proceeds through the thickness to near the weld face at the HAZ and then transversely into the weld and base metal on the root side only. This crack propagation occurred slowly with a constant overall displacement rate, which was only 50% higher than the minimum creep rate before cracking. Rapid deflection rate was only measured during the final 50 h, where it is probable that the cracking extended across the entire width of the weld.

The axial strain profiles for the root face of the high ferrite V-groove weld are illustrated in Fig. 10 from the grid measurements. The profiles are for width positions of 1 mm (0.04 in.) from the edge and at the axial centerline of the weld. The strain at the centerline increases from the ends to near mid-length and the maximum is 7.5% at 69% of the gage length at 503 h. The average axial strain is 3.6% at 503 h, and the strain profiles reflect the larger strains near the fillets. The positions of the major cracks are shown by short vertical lines and the limits are marked with a letter "C" — Fig.

Table 2—Creep-Rupture Test Data

	Loading and Overall creep												
	Load,	Stress,		Plastic deflection		Deflection[e]		Depl. rate			Total deflection		Average overall strain[e]
Spec.	lb	ksi	MPa	in.	mm	in.	mm	in./h	M/h	Time[e]	in.	mm	%
240	26,734	24.0	165	0.010	0.25	0.088	2.24	1.1 E-4	2.8 E-6	500CS	0.098	2.49	2.47P
Low ferrite						0.143	3.63	1.1 E-4	2.8 E-6	1000CR	0.153	3.89	4.17P
V-groove weld						0.165	4.19	2.2 E-4	5.6 E-6	1120T	0.175	4.44	
						0.231	5.87	1.0 E-3	2.6 E-5	1219CW	0.241	6.12	5.14P
	20,000							6.7 E-5[b]	1.7 E-6	1519[a]	0.261	6.63	
										1780R			
241	26,570	24.0	165	0.012	0.30	0.102	2.59	1.6 E-4	4.1 E-6	500CS	0.114	2.90	3.62P
Low ferrite						0.173	4.39	3.2 E-4	8.1 E-6	790T	0.185	4.70	
square groove						0.256	6.50	3.4 E-3	8.6 E-5	811CW	0.268	6.81	P
weld	13,285					+0.003	+0.07	6.8 E-6	1.7 E-7	1291[c]	0.271	6.88	
	19,928					+0.007	+1.18	2.6 E-4	6.6 E-6	1318	0.278	7.06	
						+0.045	+1.14	1.6 E-3	4.1 E-5	1358	0.323	8.20	
										1362R			P
242													
High ferrite	26,693	24.0	165	0.013	0.33	0.131	3.33	2.0 E-4	5.1 E-6	503CR	0.144	3.66	3.6P
V-groove weld						0.287	7.29	3.0 E-4	7.6 E-6	1009CS	0.300	7.62	7.7P
						0.352	8.94	4.0 E-4	1.0 E-5	1204T	0.365	9.27	
										1241R			
243	26,760	24.0	165	0.005	0.13	0.108	2.74	1.7 E-4	4.3 E-6	503CR	0.113	2.87	3.02P
High ferrite						0.213	5.41	2.5 E-4	6.3 E-6	1007CS	0.218	5.54	5.70P
square groove						0.314	7.98	3.4 E-4	8.6 E-6	1354T	0.319	8.10	8.31P
weld	20,070					+0.111	+ 2.82	1.0 E-5	2.5 E-7	2000	0.43	10.92	
						+0.613	+15.6	6.1 E-4	1.5 E-5	2403	0.73[d]	18.54	
										2418R			

(a) 300 h at reduced load, rate beginning to increase.
(b) Rupture after 561 h at final load.
(c) 480 h at 50% load.
(d) 1073 h at 75% load.
(e) T—transition at double minimum rate; R—rupture; +—additional; P—photograph of grid; CS—cracking surface weld; CR—cracking root weld; CW—complete weld crack.

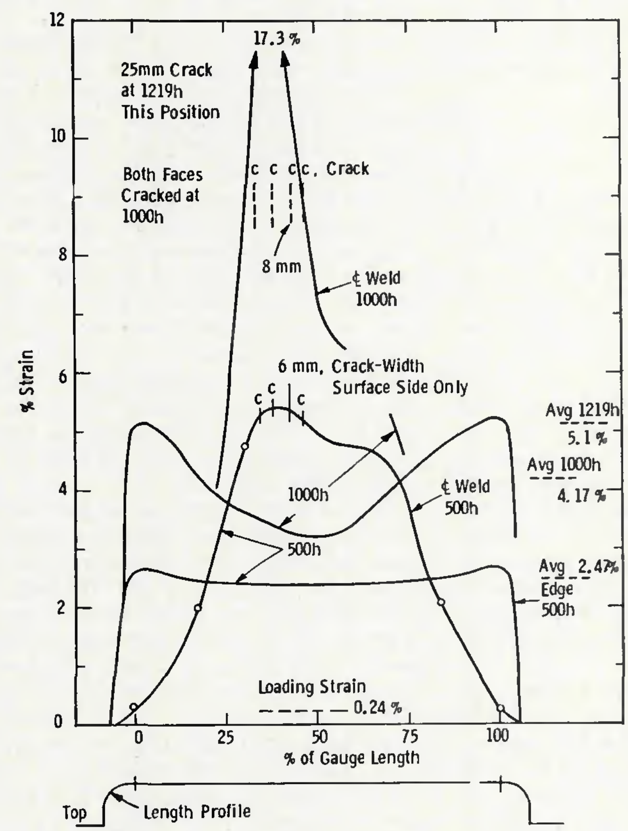

Fig. 5—Axial strain profiles of low-ferrite V-groove weld at 24 ksi (165 MPa) and 1100°F (593°C), specimen 240

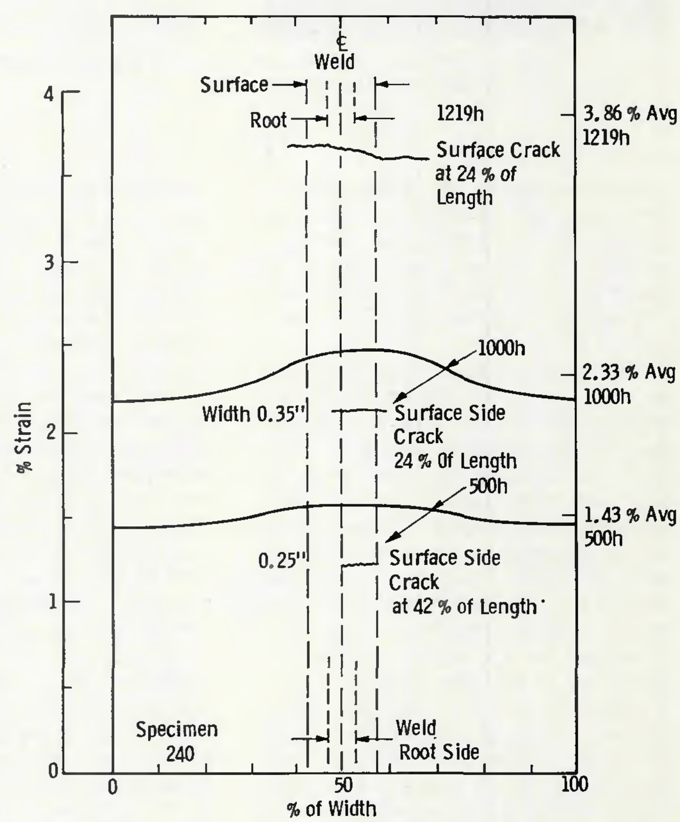

Fig. 6—Lateral strain profiles of low-ferrite V-groove weld at 24 ksi (165 MPa) and 1100°F (593°C)

10.

At 1009 h, the average axial strain is 7.7%, and the HAZ cracking has extended from 28% to 78% of the gage length where the strain is over 7.5%. The larger strains from the grid measurements reflect the openings of the cracks.

Specimen 243. The high-ferrite straight-weldment (Fig. 2) had a minimum deflection rate near 500 h and a gradual increasing rate up to 1345 h; the latter rate was double that of the minimum and is listed in Table 2 as the transition, T.

The photograph at 503 h (Fig. 11A) and visual inspection showed four cracks at the right HAZ on the root face at 51, 52, 60 and 62% of the gage length. The major cracks at 52 and 60% are shown in Fig. 11A, and the maximum crack length at 60% of length was only 1 mm (0.04 in.). No cracking was visible on the weld face.

The axial strain profiles in Fig. 12 show the characteristic behavior of axial weldments with end constraints. The axial strain for 503 h at the major crack was 6.8% at 60% of gage length.

At 1007 h (Figs. 11B and 12), extensive cracking has occurred at the HAZ's from 40% to 70% of gage length on the root face. Crack initiation was also observed

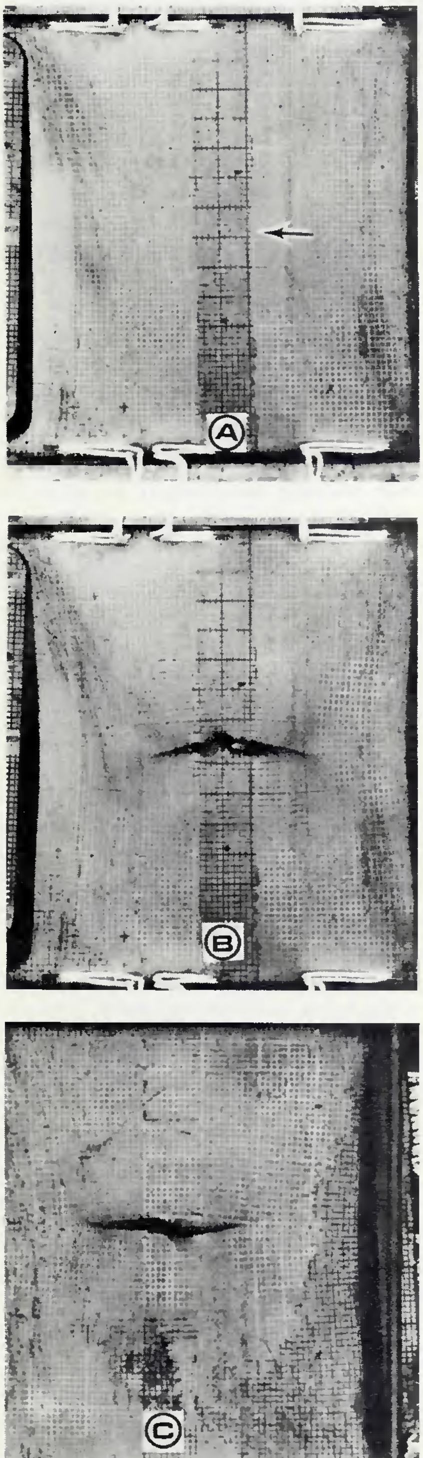

Fig. 7—Photographs of low-ferrite square groove weld, 241: A—500 h, weld face; B—811 h, weld face; C—811 h, root face

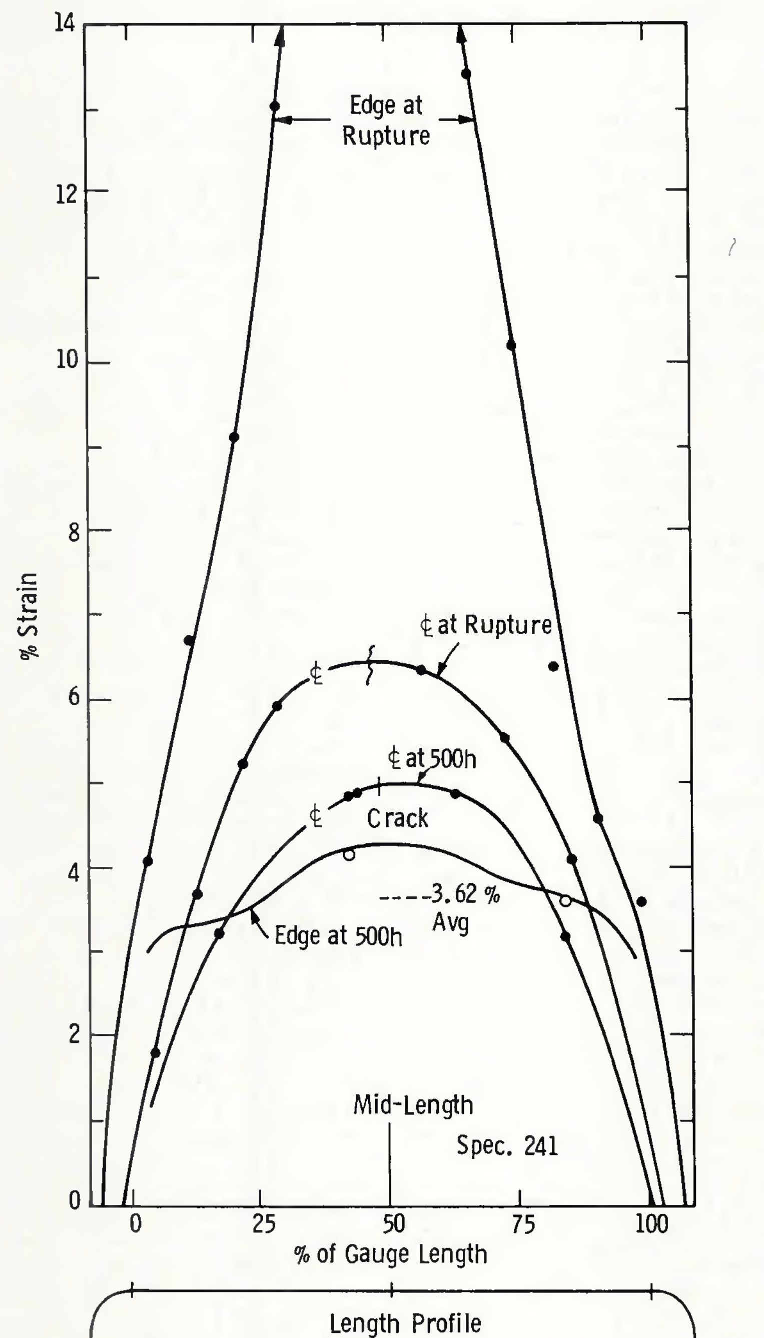

Fig. 8—Axial strain profiles for weld face of low-ferrite square groove weld at 24 ksi (165 MPa) and 1100°F (593°C)

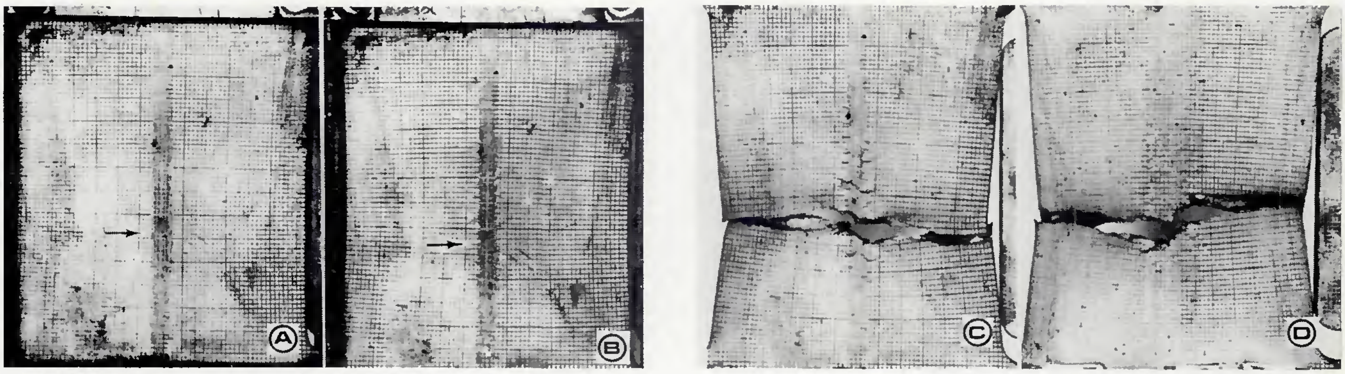

Fig. 9—Photographs of high-ferrite V-groove weld, 242: A—503 h, root face; B—1009 h, root face; C—rupture, root face; D—rupture, weld face

at the HAZ on the weld face at 60% of length—Table 2. The photograph (Fig. 11B) shows the plastic deformation bands emerging from the ends of the major crack at 60% of length at 1007 h. The crack length on the root HAZ had doubled in length to 2 mm (0.08 in.).

At 1345 h (Figs. 11C and 11D), the crack at 60% of length has extended into the weld and base metals on the root face, and many intermittent cracks have developed on the faces at all HAZ's and in the weld metal. Deformation bands with an included angle of about 75 deg are evident (Fig. 11D) on the weld face. The peak strain with crack openings is 21.8% near the weld centerline (Fig. 12), and HAZ cracking has extended from 34% to 69% of the gage length—Fig. 11.

The load was then decreased to 75% and the deflection rate decreased to 3.4% of that at the prior load—Table 2. After 175 h, the rate gradually increased with rupture after 1073 h at 75% of original load—Table 2.

Discussion

Two levels of ferrite of the Type 308 stainless steel weld metal were investigated. These levels were about 2 and 9 FN and are designated here as "low"- and "high"-ferrite. These correspond to extra-low and medium ferrite levels (Ref. 1). Two configurations of the weld were investigated: a V-groove weld with an included angle of 75 deg and a square groove weld made from one side. The V-groove weld resulted in considerable dilution at the weld root so that the ferrite number was higher at the weld root than that at the crown face for the low ferrite weldment—but lower at the root than that at the crown face for the high ferrite weldment. The stress-rupture tests were conducted at 24 ksi (165 MPa) and 1100°F (593°C).

The low-ferrite weldments showed crack initiation in the weld metal at about 4.8% axial strain on the weld face only at about 490 h. This is about 40% of the life of the V-groove weld and 60% of that for the square groove weld. The major crack grew slowly through the weld metal to the root face for the V-groove weld up to 80% of life (500 additional hours) and then accelerated across the test section. The test was interrupted at 1219 h when failure was imminent. For the square groove weld, crack growth through the weld was more rapid, and the 24 ksi (165 MPa) rupture test was terminated in 321 additional hours (811 h total time).

For the high-ferrite weldments, the crack initiation was in the HAZ on the root face at about 36% of life. The estimated strain at crack initiation was 7.5% for the V-groove weld and 6.8% for the square groove weldment. For both welds, crack growth through the HAZ to the weld face was slow during the next 34% of life (70% total). The V-groove weld ruptured at 1241 h, and the 24 ksi (165 MPa) rupture test of the square groove weld was terminated in the third stage of creep at 1345 h.

For the tests which were terminated in the third stage of creep, the load was lowered to observe the extension rate or crack growth rate in the base metal. Further analyses are necessary to estimate the crack lengths and the net section loadings at a given time.

A comparison of the rupture data with those for weld metal, base metal and the minimum data used by the ASME Code for allowable stress is given in Fig. 13. All the tests of this program gave longer lives than those for the base metal or the Code minimum data. At the rupture time of the high-ferrite square groove weld, the rupture strength of the high-ferrite square groove weld was 20% greater than that of the Code minimum data. Even for the lowest rupture time of these welds—for the low-ferrite weld—the rupture strength was 13% greater than that of the Code minimum value. The minimum crack initiation time at the stress level of these weldments is 67% longer than the corresponding rupture time for the Code minimum data.

Although the higher ferrite weld metal has a higher short-time yield strength, the creep strength at 1100°F (593°C) is lower (Ref. 1 and Fig. 13).

Failure Mechanisms

This type of testing, where all the zones of the weldment are forced to have the same average strain and strain rate, demonstrated the mechanisms of failure for the two levels of ferrite in the weld metal.

For the low-ferrite welds, the stronger weld metal assumes a higher stress during the initial loading and the redistribution of stresses with increasing creep strain.

The maximum principal stress occurs at the weld face where the initial residual stresses are also tensile. The stress state is triaxial for the initial residual stresses and practically biaxial for the applied loading. With an increase of creep strain with time, the state of stress becomes nearly biaxial. From the measurements of strain given above, the transverse stress in the weld is estimated to be about 24% of the axial stress. Crack initiation occurred in the weld metal on the surface face after about 4.8% axial strain. It is proposed that the damage for the weld face of the weld is due to the history of maximum principal stress (Ref. 7). The rupture life is determined from the accumulative damage using the stress history and the weld metal property of Fig. 13.

For the high-ferrite welds, the weld metal is more ductile and the creep strength is lower than the corresponding properties for the low-ferrite weld metal. A comparison of the creep rates at a given stress is over a factor of 10 higher for the high-ferrite weld metal (Ref. 1). Although the high-ferrite weld metal is stronger than the base metal, the difference in strength is reduced in comparison to that for the low-ferrite weld metal. Cracks were initiated in the HAZ on the weld root face after about 7% axial strain.

It is proposed that the failure mechanism for the high-ferrite weld metal is one of ductility exhaustion at the fusion line on the root face as influenced by the state of stress, the metallurgical notch and the prior working of the HAZ during the welding process (Refs. 7, 8). The state of stress at these regions is biaxial tension where the triaxiality factor (Ref. 7) is about 1.37 or about 23% reduction of ductility. The metallurgical notch is due to the cast structure of the weld adjacent to the grain growth of the heat-affected zone. The prior working by the deformations and the thermal history during the welding process cause an increase in hardness which is a maximum at the weld root face — Table 1.

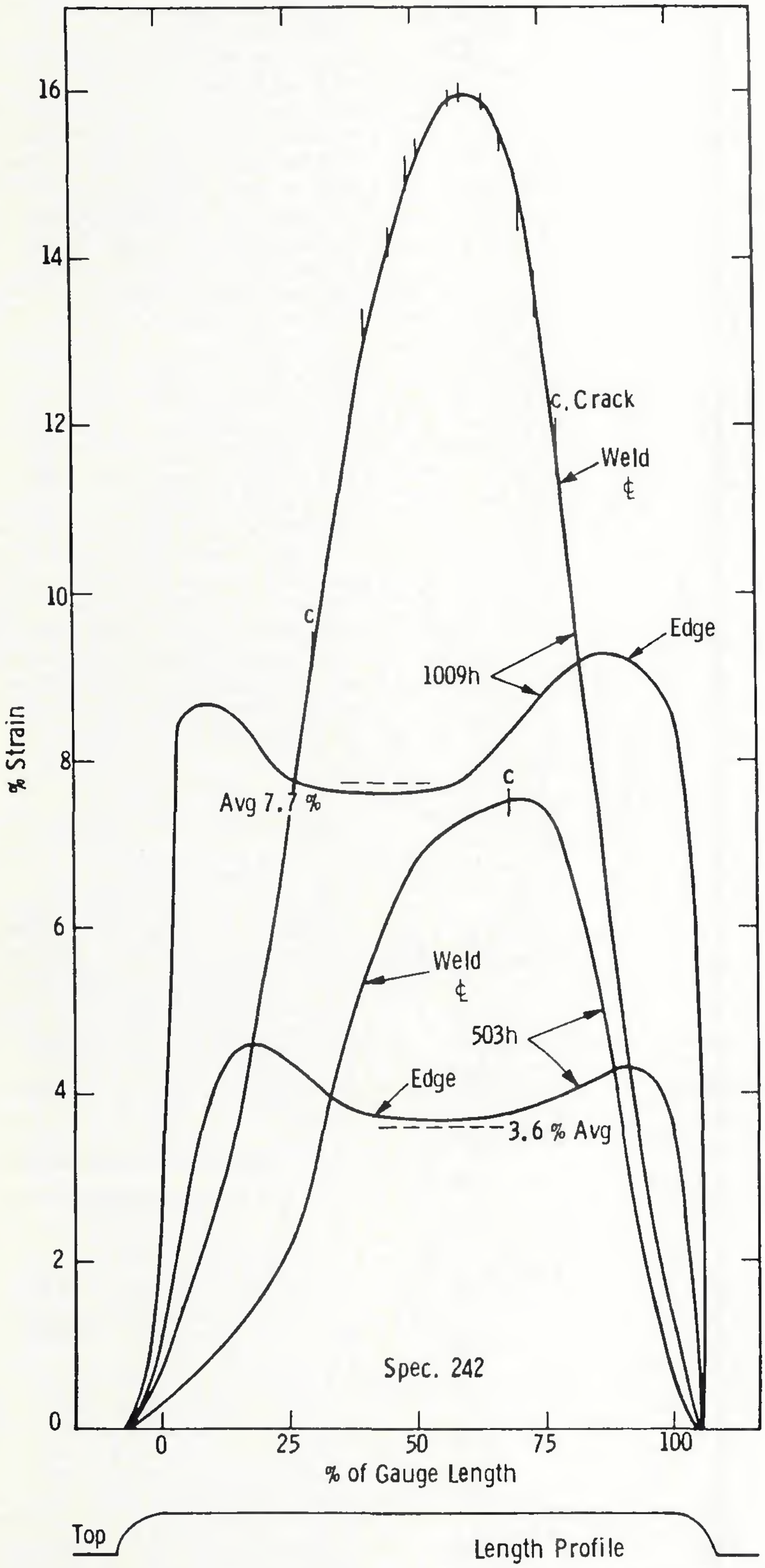

Fig. 10 — Axial strain profiles for weld root of high-ferrite axial V-groove weld at 24 ksi (165 MPa) and 1100°F (593°C)

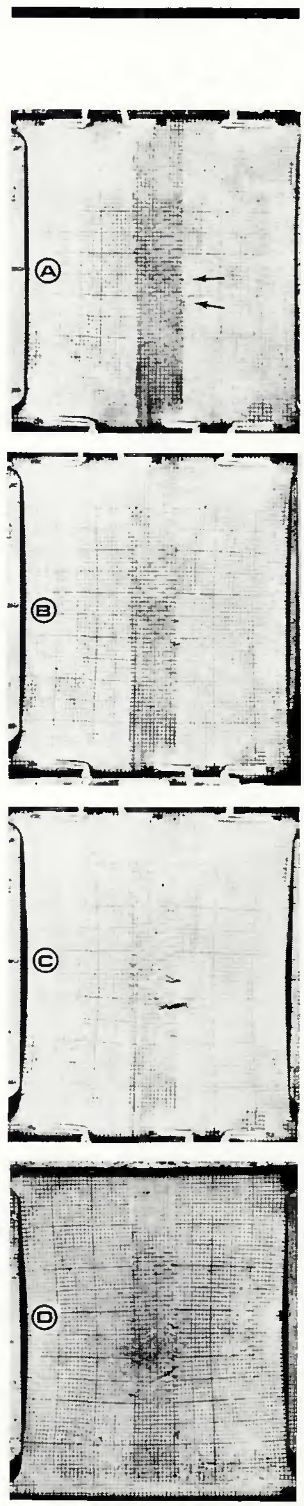

Fig. 11 — Photographs of high-ferrite square groove weld, 243: A — 503 h, root face; B — 1007 h, root face; C — 1345 h, root face; D — 1345 h, weld face

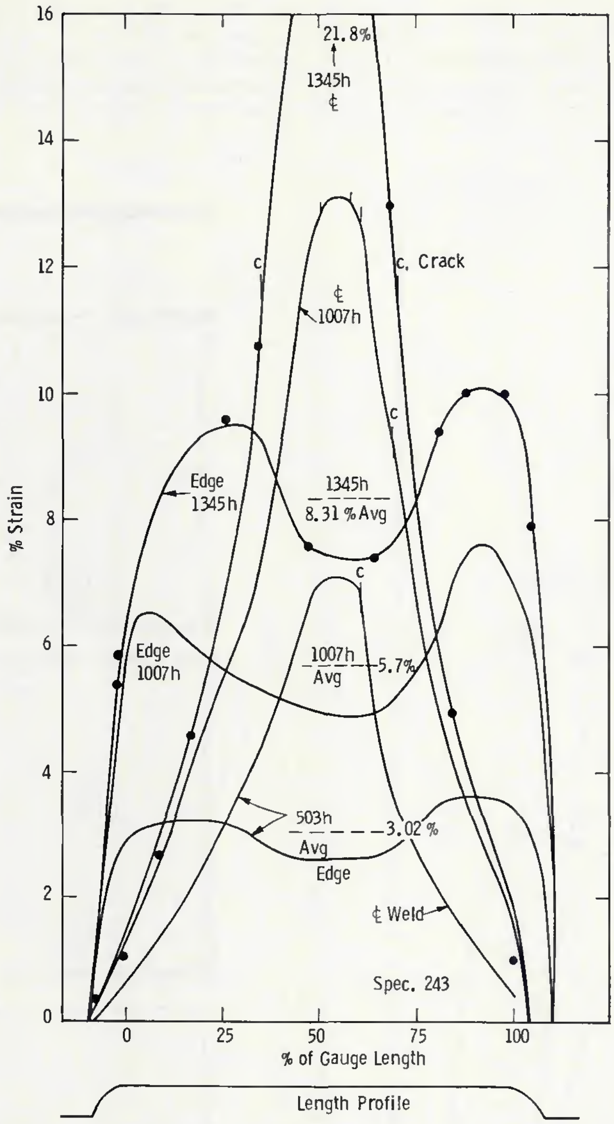

Fig. 12 — Axial strain profiles for high-ferrite axial square groove weld at 24 ksi (165 MPa) and 1100°F (593°C)

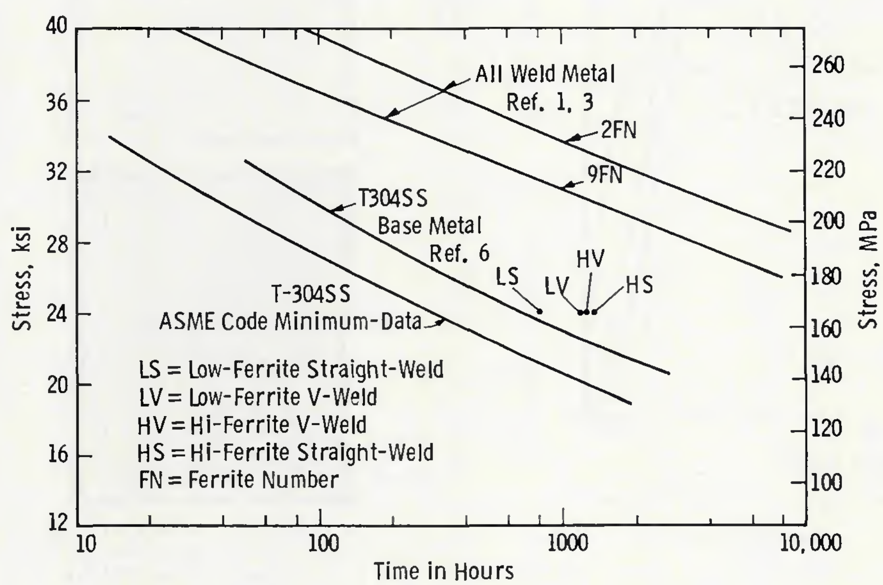

Fig. 13 — Comparison of rupture data at 1100°F (593°C)

Conclusion

Wide plates with an axial weld and end constraint were tested at 165 MPa (24 ksi) and 593°C (1100°F). This weldment test produces a constraint similar to a circumferential pipe weld where all zones of the weldment are subjected to the same overall strain.

The test weldments employed two levels of ferrite, 2 FN and 9 FN, and two weld configurations — a 75 deg V-groove weld and a square groove weld.

A low-ferrite weldment had crack initiation at about 4.8% axial strain in 490 h in the weld metal on the weld face. Crack propagation was through the weld metal to the root face and then into the HAZ and base metal. The tests were terminated in the third stage of creep at 1219 h for the V-groove and 811 h for the square groove weld.

For the high-ferrite welds, crack initiation was at about 7% axial strain in the HAZ on the root face at 36% of life and the growth through the HAZ to the surface face required the next 34% of life. The V-groove weld ruptured in 1241 h, and the square groove weld was terminated in the third stage at 1345 h.

The minimum rupture time of these tests (low-ferrite straight-weldment) is 270% of that for the Code minimum, and even the minimum crack initiation time of these weldments is 67% higher than the Code minimum rupture time.

Acknowledgments

This work was sponsored by the Metal Properties Council under the guidance of Subcommittee 1 Task Group on the Properties of Weldments in Elevated-Temperature Service. The weldments and ferrite measurements were prepared at the Oak Ridge National Laboratory under the supervision of D. P. Edmonds. The creep-rupture tests were performed at the Westinghouse Research and Development Center by E. Van Antwerp and C. Fox.

References

1. Hauser, D., and Van Echo, J. A. 1982. Effects of ferrite content in austenitic stainless steel welds. *Welding Journal* 61(2): 37-s to 44-s.

2. Manjoine, M. J. 1976. Determination of plastic or creep strains by grids. American Society for Testing and Materials, STP 608.

3. Thomas, R. D., Jr. 1978. Effect of delta ferrite content of E308-16 stainless steel weld metal — weld metal preparation. *Proc. of the symp. on properties of steel weldments for elevated temperature pressure containment applications*, G. V. Smith, Ed., pp. 1-16. Metal Properties Council publication MPC-9 (1978).

4. Hauser, D., and Van Echo, J. A. 1978.

Effect of delta ferrite content of E308-16 weld metal — mechanical properties and metallographic studies, pp. 17, 46 (1978).
5. Edmonds, D. P., Vandergriff, D. M., and Gray, R. J. 1978. Effect of delta ferrite content of E308-16 stainless steel weld metal — supplemental studies, pp. 47-61 (1978).
6. Sikka, V. K., McCoy, H. E., Booker, M. K., and Brinkman, C. R. 1975 (Nov.). Heat-to-heat variation in creep properties of Type 304 and Type 316 stainless steels. *Journal of Pressure Vessel Technology*, pp. 243-251. New York: American Society of Mechanical Engineers.
7. Manjoine, M. J. 1982. Creep-rupture behavior of weldments. *Welding Journal* 61(2): 50-s to 57-s.
8. Manjoine, M. J. 1977. Crack initiation and growth in welds at 1100°F (593°C). *Trans. 4th inter. conf. on structural mechanics in reactor technology (SMIRT)*, vol. G, paper 1/8, North-Holland Publishing Co.

WRC Bulletin 301
January 1985

A Parametric Three-Dimensional Finite Element Study of 45 Degree Lateral Connections
By P. P. Raju

This bulletin contains a summary of three-dimensional finite element studies carried out on four lateral configurations subjected independently to internal pressure, external in-plane moment on the nozzle, and external in-plane moment on the run pipe. Stress indices for various critical regions are summarized.

Publication of this report was sponsored by the Task Group on Laterals that reported to the Subcommittee on Reinforced Openings and External Loadings and the Subcommittee on Piping Pumps and Valves of the Pressure Vessel Research Committee of the Welding Research Council.

The price of WRC Bulletin 301 is $14.00 per copy, plus $5.00 for postage and handling. Orders should be sent with payment to the Welding Research Council, Room 1301, 345 E. 47 St., New York, NY 10017.

Call for Papers—
Modeling and Control of Casting and Welding

The Engineering Foundation Conference, Modeling and Control of Casting and Welding Processes, is scheduled for January 12-17, 1986, in Santa Barbara, Calif. The program will focus upon methods and applications of modeling and control to casting and welding processes. Both scientific fundamentals and practical applications will be emphasized.

Contributions from academic, industrial and government laboratories are solicited for the conference. Fundamental topics to be addressed include: evolution of microstructure; structure, stability and heat transfer at interfaces; modeling of heat transfer during welding; methods of process control and automation; surface tension and electromagnetic-force driven flow during welding, crystal growth and casting.

Submitted abstracts must be received by July 1, 1985. Send to Professor Sindo Kou, Dept. of Metallurgical and Mineral Engineering, 1509 University Ave., University of Wisconsin, Madison, WI 53706; or Dr. Robert Mehrabian, Dean of the College of Engineering, 1012 Engineering Bldg., University of California, Santa Barbara, CA 93106.

Call for Papers—
International Welding Research

Papers are solicited for the ASM/AWS/WRC-sponsored conference on "International Trends in Welding Research," to be held in Gatlinburg, Tenn., May 18-22, 1986. This eight-session symposium will cover heat and fluid flow problems in welds, solidification, solid state transformations, mechanical behavior of welds, and welding processes and process control. Conference proceedings will be published. Submit abstracts up to 300 words by November 15, 1985, to S. A. David, Materials Joining Laboratory, Metals and Ceramics Divisions, Oak Ridge National Laboratory, P. O. Box X, Oak Ridge, TN 37831. Inquiries for future information should be addressed to American Society for Metals (ASM) Conference Dept., Metals Park, OH 44073.